—Review—

Intracoronary Imaging Modalities for Vulnerable Plaques

Koji Kato[1], Masahiro Yasutake[2], Taishi Yonetsu[1],
Soo Joong Kim[3], Lei Xing[1], Christina M Kratlian[1],
Masamichi Takano[4], Kyoichi Mizuno[2] and Ik-Kyung Jang[1]

[1]Cardiology Division, Massachusetts General Hospital and Harvard Medical School, USA
[2]Department of Internal Medicine, (Division of Cardiology, Hepatology, Geriatrics and Integrated Medicine), Nippon Medical School
[3]Department of Cardiology, College of Medicine, Kyung Hee University, Seoul, Korea and Cardiology Division, Massachusetts General Hospital and Harvard Medical School, USA
[4]Cardiovascular Center, Nippon Medical School Chiba Hokusoh Hospital

Abstract

The concept of vulnerable plaque (VP) has been widely accepted as the primary cause of acute coronary syndrome (ACS) and sudden cardiac death. ACS is thought to result from sudden disruption of a VP with subsequent occlusive thrombosis. VP typically consists of several components; a large necrotic core, thin fibrous cap, increase in macrophage activity, increase in vaso vasorum, and positive remodeling.

In recent years, invasive or non-invasive diagnostic imaging modalities have been developed for indentifying VP. VP has been recognized in various modalities not only by visualization of cross sectional images by high-resolution imaging modalities, such as virtual histology intravascular ultrasound (VH-IVUS), integrated backscatter (IB) IVUS, and optical coherence tomography (OCT), but also by direct visualization by intracoronary angioscopy.

VH-IVUS uses advanced radiofrequency signal analysis of ultrasound signals and allows detailed qualitative and quantitative assessment of plaque composition, while IB-IVUS analyzes the radiofrequency signal by applying a fast Fourier transformation of the component of the backscattered signals. Different tissue components reflect the radiofrequency signaling at different power levels, which could be used to differentiate various tissue components. Angioscopy allows direct visualization of internal surface of the lumen, providing the detailed information of characteristics of plaque and thrombus. Optical coherence tomography (OCT) is an analog of IVUS, but uses light instead of sound. OCT has a 10-fold higher image resolution (10–15 μm) compared to conventional IVUS, therefore it is able to provide superior image quality. The commercially available versions of the technology used time-domain (TD) OCT (M2, M3, Lightlab, Westford, MA, USA) and fourier-domain (FD) OCT (C7XR, Lightlab, Westford, MA, USA). OCT is the only imaging modality with high enough resolution to measure fibrous cap thickness and neovascularization. Moreover OCT has a unique ability of detecting macrophages.

In this review, we attempted to summarize the advantages and limitations of the currently available intravascular modalities.
(J Nippon Med Sch 2011; 78: 340–351)

Key words: vulnerable plaque, virtual histology intravascular ultrasound (VH-IVUS), integrated backscatter intravascular ultrasound (IB-IVUS), angioscopy, optical coherence tomography (OCT)

Correspondence to Ik-Kyung Jang, MD, PhD, Cardiology Division, Massachusetts General Hospital, 55 Fruit St. GRB 800, Boston, MA 02114, USA
E-mail: ijang@partners.org
Journal Website (http://www.nms.ac.jp/jnms/)

Introduction

The concept of vulnerable plaque has been widely accepted as the primary cause of acute coronary syndrome (ACS) and sudden cardiac death[1]. *In vitro* pathological studies demonstrated that most cases of ACS are thought to result from sudden luminal obstruction or narrowing caused by thrombosis as a consequence of rupture or erosion of plaques or superficial calcified nodule[2–4]. VP is not only lipid-rich plaque, but all types of atherosclerotic plaques with high likelihood of thrombotic complications[2,3]. In recent years, invasive or non-invasive diagnostic imaging technologies have been developed for indentifying VPs. VP is classified by three different types (rupture, erosion and calcific nodule)[5]. Retrospective pathologic studies suggest that active inflammation with infiltration of monocytes, macrophages, or T-lymphocytes[6–8], thin fibrous cap (≤65 mm) with a large lipid core (thin capped fibroatheroma: TCFA)[9,10] and positive remodeling are indicators of plaque rupture with thrombus[3,11]. And the plaque erosion with thrombus suggests that the plaque is often rich in proteoglycans, but, in most cases, lacking a distinguishing structure such as a lipid pool or necrotic core. If a lipid-rich core is present, the fibrous cap is usually thick and rich in smooth muscle cells[9]. These plaques are often associated with constrictive remodeling. The plaques with thrombus covering a calcified nodule are appearing to be heavily calcified nodule protruding into the lumen with the loss and/or dysfunction of endothelial cells[9]. While such plaques are highly suspected to be ones at risk of thrombosis, they cannot be designated as such until prospective studies provide the necessary supporting data[5]. Major advances in coronary artery disease prevention will require early detection of vulnerable plaques. It is important to further identify the high-risk plaques before their disruption and formation of occlusive thrombus.

Coronary angiography is used as the 'gold standard' for interventional therapy. However, it can only visualize a two dimensional silhouette of coronary lumen and does not provide any information about the characteristics of the arterial wall contents. For this reason, coronary angiogram is not capable of detecting VP. Various histological plaque components have been targeted for detection of VP. The features and comparisons of the invasive imaging modalities are listed in the **Table 1**[12]. TCFA, considered to be *in vivo* VP, has come to be recognized by further refinement of imaging technologies such as integrated backscatter intravascular ultrasound (IB-IVUS), virtual histology IVUS, and optical coherence tomography (OCT). Angioscopy allows direct visualization of the internal surface of the lumen, providing detailed information about the characteristics of plaque and thrombus. At present, the intravascular modalities can potentially distinguish between vulnerable plaques and stable

Table 1 Comparison of Invasive Diagnostic Modalities for Detection of Vulnerable plaques

Imaging Modality	Resolution (μm)	Penetration	Fibrous cap	Lipid core	Inflammation	Calcium	Thrombus	Current Status
Grayscale IVUS	150-250	Good	+	+	−	+ + +	+	CS/CA
VH-IVUS	200-250	Good	+	+ +	−	+ + +	+	CS/CA
IB-IVUS	150	Good	+	+ +	−	+ + +	+	CS
Angioscopy	10-50	None	+	+ +	−	−	+ + +	CS/CA
OCT	10-15	Poor	+ + +	+ + +	+	+ +	+ +	CS/CA

IVUS; intravascular ultra sound
VH-IVUS; virtual histology IVUS
IB-IVUS; integrated backscatter IVUS
OCT; optical coherence tomography
CS; clinical studies
CA; indicates clinical approved for commercial use

Modified from Suh WM et al, Circ Cardiovac Imaging 2011; 4 (2); 169-78

plaques. In this review, we attempted to summarize the advantages and limitations of the currently available intravascular imaging modalities.

IVUS

Grayscale IVUS

Conventional grayscale IVUS can visualize real-time high fidelity images of the entire vessel, and has been considered standard intracoronary imaging. The IVUS is ideally suited to provide accurate measurements of lumen and vessel diameters and area that allows for accurate diagnosis of obstructive coronary disease and treatment with coronary intervention. It uses the amplitude of the backscattered echo signal to differentiate highly echogenic components (calcium, dense fibrous tissue) from echolucent ones (lipid, necrotic core). The American College of Cardiology Clinical Expert Consensus Document for IVUS imaging has described that a VP can appear as an echolucent plaque[13]. In a prospective study, patients who developed ACS during a 2 year follow-up period were correlated with large echolucent area in the eccentric plaques at the time of their first study[14]. These plaques had histological features similar to vulnerable plaques and were associated with increased risk of instability. Additionally, IVUS provided detailed information on the morphology of coronary plaque and the vessel response to atherosclerosis such as remodeling, which may help to identify plaques at high risk of spontaneous rupture[15]. However, a recent study showed that IVUS *per se* was unable to distinguish fibrous from fatty plaque[16]. Moreover, the resolution of conventional IVUS is not high enough (100–150 μm) to identify microstructure such as fibrous cap, and therefore is limited in determining VP.

VH-IVUS

VH-IVUS uses advanced radiofrequency analysis of ultrasound signals and allows detailed qualitative and quantitative assessment of plaque composition. *Ex-vivo* studies have demonstrated that power spectrum-related parameters from raw backscattered ultrasound signal allow a more detailed analysis of the vessel components to identify different tissue morphology[17]. These parameters are used in classification scheme to generate a tissue map of the plaque components: fibrous (dark green), fibrofatty (yellow-green), necrotic core (red), and dense calcium (white) **(Fig. 1)**[18]. VH-IVUS data are collected during a single IVUS pullback using the volcano Eagle Eye Gold Catheter (Volcano Corporation; Rancho Cordova, CA).

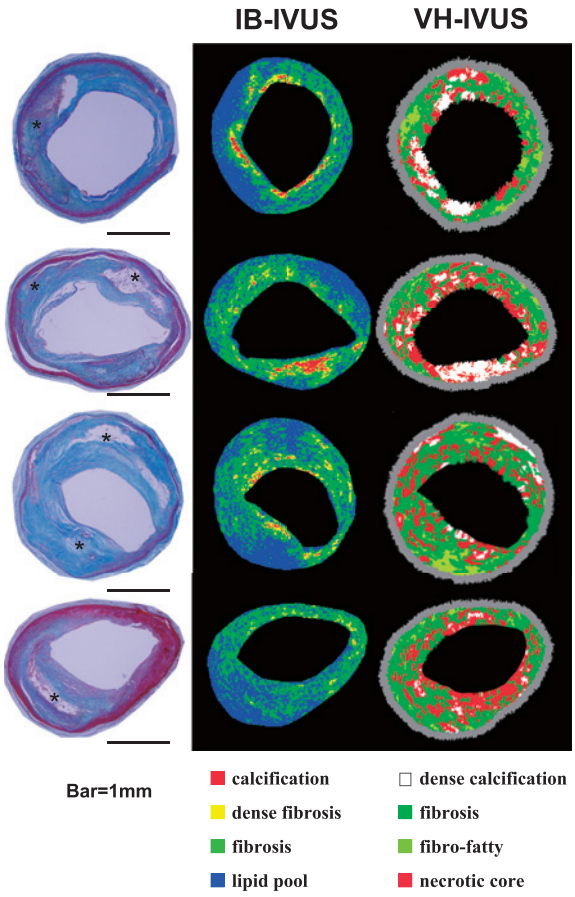

Fig. 1 TCFA with a large lipid core
Left: Histological image (Masson trichrome staining), *Lipid pool. Bar=1 mm
Middle: Corresponding color-coded maps constructed by an IB-IVUS system.
Right: Corresponding VH-IVUS images.
Reproduced with permission from Okubo et al.[18]

The accuracy of VH-IVUS algorithm validated against histology was 90.4% for fibrous tissue, 92.8% for fibro-fatty, 90.9% for dense calcium, and 89.5% for necrotic core[19]. It has been reported that in a directional coronary atherectomy study of 30 patients, correlation of VH-IVUS analysis with histopathology showed a high accuracy. The

predictive accuracy for correlation analysis between the VH image and the *in vitro* histological section was 87.1%, 88.3%, and 96.5% for fibrosis, necrotic core and calcium, respectively[20]. In clinical study, VH-IVUS has been used *in vivo* to document regression on the fibrofatty composition and plaque volume after treatment with statins[21]. Another study reported that necrotic core volume measured by VH-IVUS clearly predicted distal embolization and no-reflow phenomenon after coronary intervention in the patients with ST elevation myocardial infarction[22].

Although the axial resolution of VH-IVUS is too low (250 μm in phased array) to clearly visualize a thin fibrous cap of <65 μm thickness, the use of VH-IVUS has been tried to detect vulnerable plaques. VH-IVUS-derived TCFA has instead been defined as a necrotic core-rich (≥10%) plaque without evident overlying fibrosis tissue and with a percent plaque volume of ≥40% seen on at least 3 consecutive frames[23]. Using this definition, the sensitivity, specificity, and positive and negative predictive values of VH-IVUS to identify TCFA as determined by OCT were 89%, 86%, 59% and 97%, respectively[24]. In a clinical study, VH-IVUS-derived TCFA has been found more frequently in patients with ACS than in those with stable angina. In the larger study of 318 patients for culprit lesions, the percentage of unstable lesions (ruptured plaques or VH-IVUS-derived TCFA) was significantly greater in ACS patients than in stable angina patients (89% versus 62%; P<0.001)[25]. Another study showed VH-IVUS-derived TCFA was also more frequently observed in non-culprit lesion in the ACS patients compared with stable angina patients (64.6% versus 35.7%, P= 0.006)[26]. Moreover, the recently presented results of the Providing Regional Observation to Study Predictors of Events in Coronary Tree (PROSPECT) trial provided the first prospective natural history of vulnerable plaques observed by gray-scale IVUS and VH-IVUS. In this study, 697 patients with ACS underwent three vessel coronary angiography and IVUS study after percutaneous coronary intervention. In follow-up, recurrent clinical events were equally attributable to the culprit and nonculprit lesions (12.9% versus 11.6%). Independent predictors for clinical events such as cardiac death, arrest, or myocardial infarction from nonculprit lesions were TCFA (hazard ratio, 3.90; p=<0.001), TCFA with a minimal luminal area <4.0 mm^2 (hazard ratio, 6.55; p<0.001), TCFA with plaque burden ≥70% (hazard ratio, 10.83; p<0.001), and TCFA with a minimal luminal area <4.0 mm^2 and plaque burden ≥70% (hazard ratio, 18.2; p<0.001)[27] which were all derived from VH-IVUS. Although IVUS and VH-IVUS were able to predict clinical events, the majority of the events were unstable angina rather than cardiac death, arrest or MI.

IB-IVUS

Another technique for tissue characterization of plaque composition developed using IVUS imaging is integrated backscatter (IB)-IVUS. IB-IVUS analyzes the radiofrequency (RF)-signals generated by the 40 MHz mechanically rotating IVUS catheters by applying a fast Fourier transformation of the frequency components of the backscattered signals calculating the intensity of the signal measured in decibels (dB). Different tissue components reflect the radiofrequency signaling at different power levels, which could be used to differentiate various tissue components. IB tissue maps were originally constructed by comparing the IVUS pullback images on 18 *ex vivo* autopsy coronary segments, with their histological findings. From this work, IB-IVUS maps were divided into 5 categories; calcification, mixed lesion, fibrous tissue, lipid core, intimal hyperplasia and thrombus[28]. IB values for the various plaque components can then be calculated to construct color-coded IB-IVUS maps (**Fig. 1**)[18]. An autopsy-based study of 42 coronary specimens showed that the sensitivity of IB-IVUS for calcification, fibrous and lipid-rich plaque was 100%, 94% and 84%, respectively, and one of OCT for them was 100%, 98% and 95%, respectively, and in the case of conventional IVUS it was 100%, 93% and 67%, respectively. On the other hand, the specificity for calcification, fibrous and lipid-rich plaque of IB-IVUS was 99%, 84% and 97%, respectively, in OCT was 100%, 94%, and 98%, respectively, and in conventional IVUS was 99%, 61%, and 95%, respectively, all of them being comparable among

the 3 modalities[29]. In clinical studies, IB-IVUS has been demonstrated to be able to assess the relevant details of clinical situations and coronary plaque characteristics. IB-IVUS analysis revealed that not only culprit lesions[30] but also non-culprit lesions[31] in ACS are significantly associated with the increase in lipid component and decrease in fibrous component, and that positive remodeling with high total lipid volumes are observed in ACS lesions[32]. Furthermore, the observational serial change study of IB-IVUS demonstrated the reduction of plaque volume and lipid components and increase in fibrous tissue content in the ACS patients treated with statin therapy. This suggests that statin therapy is able to change vulnerable plaques detected by IB-IVUS into more stable plaques[33,34].

Although IB-IVUS has been developed and recently commercialized in Japan, it has some limitations. IB-IVUS is not sufficiently sensitive to distinguish intimal hyperplasia from lipid pool because both have similar IB values. Moreover, if calcification is present in the fibrous cap or in the mixed lesion, it is difficult to obtain a precise IB-IVUS image in the outside tissue because of the attenuation phenomenon[28,35]. As a consequence, IB-IVUS is unlikely to detect subtle changes in plaque composition that occur over small distances.

Angioscopy

Intracoronary angioscopy is an endoscopic technique that allows direct visualization of the internal surface of a vessel and provides detailed information regarding plaque morphology and thrombus in living patients with high resolution (10–50 μm). Endoluminal irregularities, such as ulceration, fissures, and tears, can also be seen. On the basis of angioscopic images, plaque is defined as a non-mobile, elevated, and/or protruding structure that can be clearly demarcated from the adjacent vessel wall.

A normal coronary artery appears as glistening white, whereas atherosclerotic plaque can be categorized as yellow or white. The intensity of yellow color is also an indicator of fibrous cap thickness, with high yellow intensity associated with thin, fibrous caps overlying a lipid core. Yellow intensity (or grade) of the plaque is classified semi quantitatively as 0, white; 1, light yellow; 2, (medium) yellow; or 3, dark yellow (**Fig. 2**). The majority of yellow plaques are composed of lipid rich tissue or necrotic core indentified by OCT and IVUS[28,36–39]. In contrast, white plaque is histological fibrous plaque or lipid plaque with thick fibrous cap[28,37,39]. **Figure 3** shows the relationship between color grade by angioscopy and the fibrous cap thickness measured by OCT. Yellow intensity is negatively correlated with fibrous cap thickness, the sensitivity and specificity of the angioscopy identifying yellow plaques with a fibrous cap <110 μm measured by OCT was 98% and 96%, respectively[37]. Intense yellow plaque corresponds to TCFA, and 80% of intensive yellow plaque was TCFA[37,39]. Furthermore, yellow plaque is associated with the prevalence of positive remodeling and thrombus formation[37,40]. In patients with ACS, yellow plaques were frequently observed in the culprit lesions[41–44], as well as in the nonculprit lesions[45], but angioscopically evident thrombus was present only in the culprit lesions[46]. On the other hand, stable white plaques without thrombus were seen in the ischemic-related lesions of stable angina[40]. Moreover, prospective studies demonstrated that patients having glistening or intense yellow showed higher incidence of ACS in comparison with those without yellow plaques.[47,48], These facts indicate that yellow plaque identified by angioscopy, especially intense or glistening yellow plaque, might be potentially vulnerable and increase the risk of cardiovascular events. According to the morphology, the plaque is divided into stable plaque, with smooth surface, or complex plaque, with an irregular surface. The complex plaque includes ruptured plaque, eroded plaque, intimal flap, fissure, and ulceration. Thrombus is presented as a superficial, intraluminal, or protruding mass adherent to the vessel surface but clearly a separate structure that persisted despite being flush with a saline (or Ringer's lactate) solution, and its color can be coalescent red, white coalescent red, white, mixed (white and red), or pinkish-white (**Fig. 2**).

There are some limitations of angioscopy. First, it observes only surface of the coronary lumen.

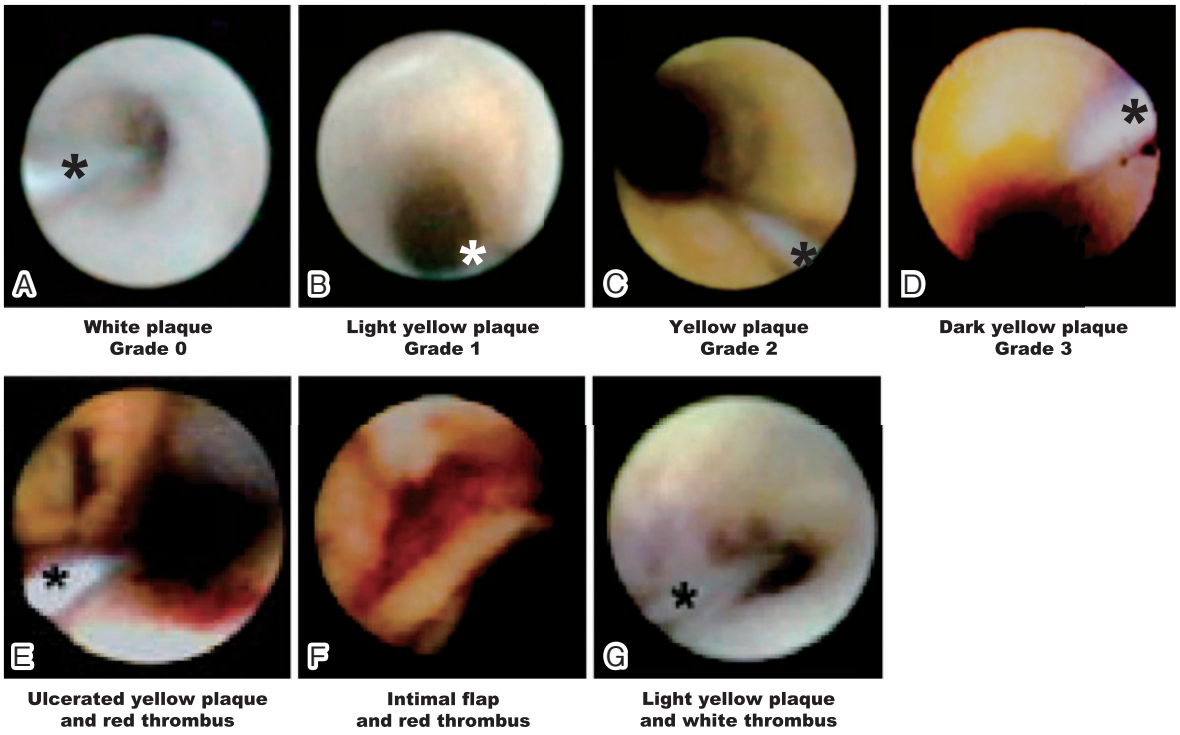

Fig. 2 Classification of coronary plaque.
(A) A white plaque (yellow grade 0). (B) A light yellow plaque (grade 1). (C) A medium yellow plaque (grade 2). (D) A dark yellow plaque (grade 3). (E) Ulcerated yellow plaque and red thrombus. (F) Intimal flap and red thrombus. (G) Light yellow plaque and white thrombus

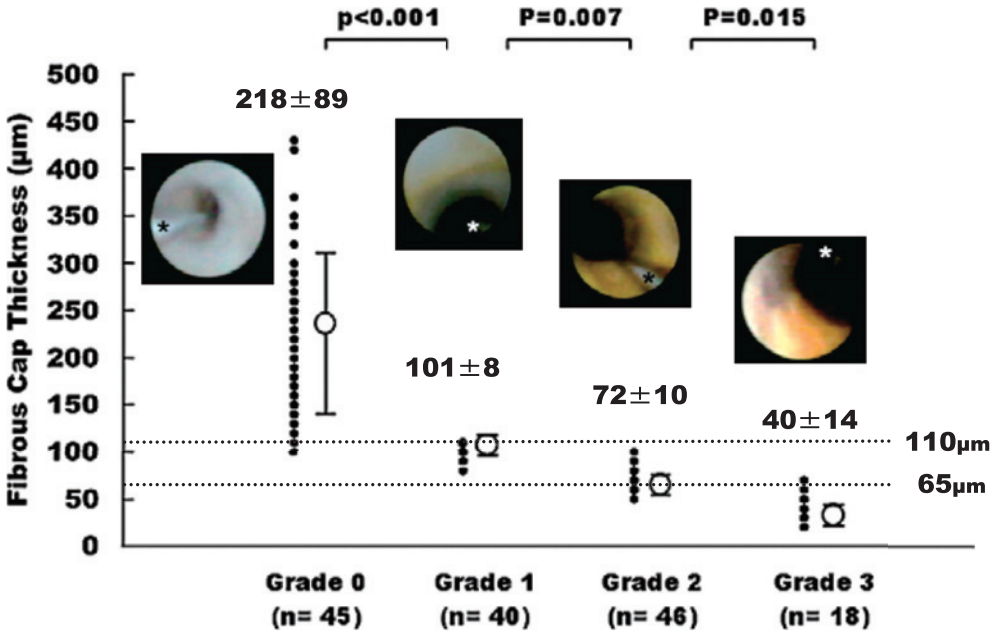

Fig. 3 Angioscopic Yellow Grade
Relationship between the angioscopic yellow grade and the fibrous cap thickness measurement by optical coherence tomography (OCT) are shown. The fibrous cap thickness by OCT decreased as yellow grade was increased.
Reproduced with permission from Takano et al.[37]

Second, it is impossible to evaluate the angioscopic findings quantitatively. In angioscopic analysis, the advantage is the ability to detect coronary thrombus more sensitively than other imaging modalities[49],

whereas the largest disadvantage is difficulty in quantitative assessment for color, distance or volume. Methods of image quantification, such as quantitative colorimetric analysis, have been developed to overcome the limitations inherent in angiocscopic images[50–52]. This may change the subjective angioscopic data so that it is more objective and reproducible. In addition, the latest *in vitro* study indicates that by using color fluorescent angisocopy, the yellow coronary plaques can be further classified into green, white-to-light blue, and yellow-to-orange plaques according to their components, such as collagen subtypes, oxidized LDL, macrophage foam cells and calcium[53]. Thus, more objective information to identify VPs will be provided in the future.

OCT

Optical coherence tomography (OCT) is an analog to IVUS, but uses light instead of sound. The light source used for OCT imaging is in the near-infrared range, around 1,300 nm wavelength. OCT has a 10-fold higher image resolution (10–15 μm) than conventional IVUS, so it is able to provide superior intraluminal image quality. The commercially available versions of this technology used time-domain (TD) detection (M2, M3, Lightlab, Westford, MA, USA). TD OCT employed a broad-band light source with wavelengths around 1,300 nm. The currently available system uses a much higher speed method, known as frequency or Fourier-domain (FD) detection (C7XR, Lightlab, Westford, MA, USA). FD OCT emits light at wavelength of 1,250–1,350 nm onto the vessel wall, and an image can be obtained using interferometer through recording the backscattering of light from the vessel wall.

OCT provides high resolution of 10 μm, which allows it to identify various components of atheromatous plaques. Normal coronary artery walls appear as a three-layer structure in OCT images. The vascular media is seen as a dark band delineated by the internal elastic lamina and external elastic lamina (**Fig. 4-A; arrow**). Fibrous plaques consist of homogeneous high back-scattering areas (**Fig. 4-B**)[54–58]. Lipid-rich plaques exhibit lower signal density and more heterogeneous back-scattering than fibrous plaques. There is a strong contrast between lipid-rich cores and fibrous regions on OCT images. Therefore, the lipid-rich core most often appears as diffusely bordered, signal-poor regions (lipid pool) with overlying signal-rich bands that correspond to fibrous caps (**Fig. 4-C; arrows**)[54–58]. Calcified plaques are identified by the presence of well-delineated, low back-scattering, heterogeneous regions (**Fig. 4-D**)[54–58]. Superficial micro-calcifications, considered to be a distinctive feature of plaque vulnerability, are revealed as small superficial calcific deposits. In an initial study by our group, a qualitative image classification scheme was developed based on correlation of OCT images with histological images. The sensitivity and specificity of identification of fibro-calcific plaque, and lipid tissue were 96%, 97% and 90%, 92%, respectively. For fibrous plaque, the sensitivity was lower (79%), but specificity remained high (98%)[54]. Subsequently, we applied the same criteria to *in vivo* imaging[55]. OCT observational study in the patients with acute and stable coronary disease demonstrated that plaque characteristics were associated with different clinical presentations. Lipid-rich plaque (defined by lipid occupying $\geq$2 quadrants of the cross-sectional area) was observed in 90% of patients with STEMI, 75% of patients with NSTEMI or unstable angina, and 59% of patients with stable angina[57]. And also lipid-rich plaque identified by OCT has been associated with an increase in incidence of post-procedural cardiac enzyme elevation or no reflow phenomenon in the patients with not only with ACS, but also with stable angina[59,60].

Among all intravascular imaging diagnostics, OCT is the only modality with high enough resolution to measure thickness of the fibrous cap. TCFA is defined pathologically as a lipid core covered by a fibrous cap with a thickness <65 μm, with infiltration of inflammatory cells[9,10]. In OCT observational studies *in vivo*, TCFA was detected in 72% STEMI and 50% NSTEMI culprit lesions as compared to 20% SAP (P=0.01) lesions, and measurement of fibrous cap thickness were 47, 54 and 103 μm, respectively[57]. Moreover, the presence of TCFA is

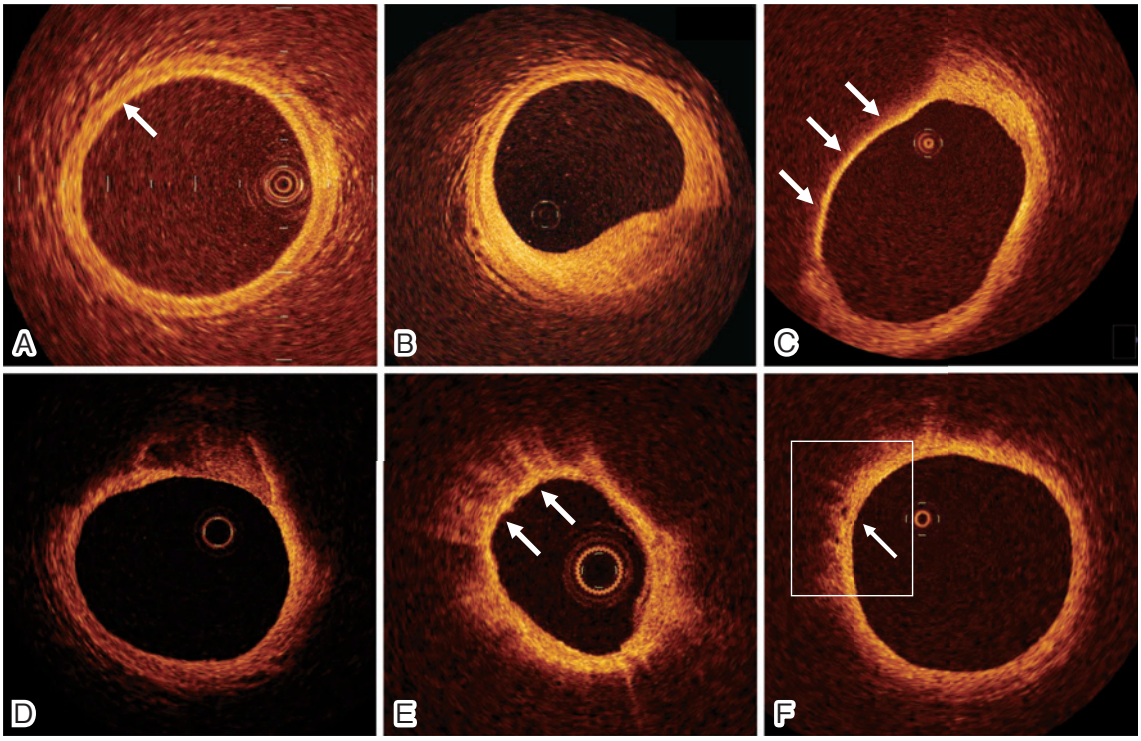

Fig. 4 OCT images

(A) Normal coronary
The vascular media is seen as a dark band delimited by the internal elastic lamina and external elastic lamina **(arrow)**.

(B) Fibrous plaque
Fibrous plaque is observed as homogenous high back-scattering area.

(C) Lipid-rich plaque
Lipid-rich plaque is observed as diffusely bordered, signal-poor regions with overlying signal-rich bands that correspond to fibrous cap **(arrows)**.

(D) Calcified plaque
Calcium is observed as well-delineated, low back-scattering, heterogeneous regions.

(E) Macrophage
Macrophages are observed as a bright spot with a high signal variance from the surrounding tissue **(arrows)**.

(F) Neovasculization
Neovascularization is observed as microchannel with tiny black hole **(arrow)**.

an independent risk factor of post-PCI procedural MI[60] and major adverse cardiac event (MACE)[61]. Plaque disruption is common finding associated with ruptured plaques visualized by OCT. It can be observed as a ruptured fibrous cap that connects the lumen with the lipid pool **(Fig. 5-A)**. Plaque disruption has been found more frequently in AMI patients (73%) than in SAP patients (12%)[56,57].

Another strength of OCT is the ability to identify coronary thrombus. Thrombus is identified as masses protruding into the vessel lumen from the surface of the vessel wall. Red thrombus consists mainly of red blood cells; relevant OCT images are characterized as high-backscattering protrusions with signal-free shadowing **(Fig. 5-B)**. White thrombus mainly consists of platelets and is characterized by signal-rich, low-backscattering billowing projections protruding into the lumen **(Fig. 5-C)**[62,63].

Moreover, the unique ability of OCT is the detection of macrophages, which are relatively large (20 to 30 μm) cells and contain multiple lipid-rich bodies. Degradation of the fibrous cap matrix by macrophages is an important contributor to atherosclerotic plaque instability[8]. Such macrophages can be observed directly by OCT as a 'bright spot',

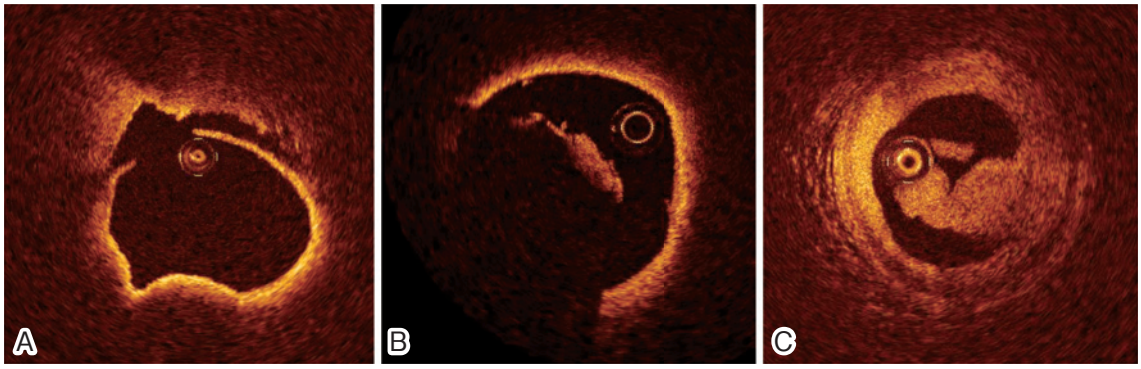

Fig. 5 OCT images

(A) Plaque disruption
Plaque disruption is observed as a tear of fibrous cap that connects the lumen with the lipid pool.
(B) Red thrombus
Red thrombus is observed as high-backscattering protrusions with signal-free shadowing.
(C) White thrombus
White thrombus is observed as signal-rich, low-backscattering billowing projections protruding into the lumen.

(Fig. 4-E; arrows) with a high signal variance from the surrounding tissue[64]. The macrophage foam cells are detectable and quantified with high accuracy. In an autopsy study, OCT images of 26 lipid-rich segments were correlated with histology, and OCT was able to detect a cap macrophage density > 10% with 100% sensitivity and specificity[64].

OCT has the potential to identify neovascularization as microchannels with tiny black holes (50−100 μm) **(Fig. 4-F; arrow)**. Plaque neovascularization has been identified recently as a common feature of plaque vulnerability[65], and increasing microchannel counts correlated with a greater frequency of TCFA[66]. An observational study of OCT revealed that the presence of microchannels in the plaques is associated with thinner fibrous cap, positive remodeling, and elevated hs-CRP levels[67]. OCT has been proposed as a high resolution imaging modality that can identify microstructures in atherosclerotic plaques, and so might provide an opportunity to directly detect plaque neovascularization *in vivo*.

The major limitations of OCT are poor tissue penetration and interference from blood, which derive from its use of light-based energy source. OCT has a penetration depth of 2 to 3 mm, which prohibits images of outside the internal elastic lamina. Blood should be displaced before OCT imaging by saline, lactate Ringer solution, Dextran, or contrast medium infusion. An additional limitation is that differentiation of certain plaque characteristics is still difficult. It is not always easy to distinguish lipid from calcium. Both lipid and calcium create signal-poor regions, and the only difference is the border characteristics (lipids have diffuse borders, and calcium has sharp borders)[68]. Comparison studies with other imaging modalities may be helpful in improving the diagnostic criteria between lipid and calcium.

Conclusion

A number of different novel imaging modalities have been investigated to define the specific characteristics of vulnerable plaque. However, most of these techniques are still undergoing refinement and cannot reliably identify vulnerable plaque in the clinical situation. The combination of different technologies, including imaging, physiological tests, and serum/genetic tests, may make it possible to detect vulnerable plaque. Many unanswered questions remain, however, there is a real clinical proposition to understand the natural history of these vulnerable plaques. These efforts will hopefully enable us to prevent plaque rupture and lead us to an era of primary prevention even in the field of interventional cardiology in the future.

References

1. Falk E, Shah PK, Fuster V: Coronary plaque disruption. Circulation 1995; 92: 657–671.
2. Naghavi M, Libby P, Falk E, et al.: From vulnerable plaque to vulnerable patient: a call for new definitions and risk assessment strategies: Part I. Circulation 2003; 108: 1664–1672.
3. Naghavi M, Libby P, Falk E, et al.: From vulnerable plaque to vulnerable patient: a call for new definitions and risk assessment strategies: Part II. Circulation 2003; 108: 1772–1778.
4. Virmani R, Kolodgie FD, Burke AP, et al.: Atherosclerotic plaque progression and vulnerability to rupture: angiogenesis as a source of intraplaque hemorrhage. Arterioscler Thromb Vasc Biol 2005; 25: 2054–2061.
5. Schaar JA, Muller JE, Falk E, et al.: Terminology for high-risk and vulnerable coronary artery plaques. Report of a meeting on the vulnerable plaque, June 17 and 18, 2003, Santorini, Greece. Eur Heart J 2004; 25: 1077–1082.
6. Kovanen PT, Kaartinen M, Paavonen T: Infiltrates of activated mast cells at the site of coronary atheromatous erosion or rupture in myocardial infarction. Circulation 1995; 92: 1084–1088.
7. van der Wal AC, Becker AE, van der Loos CM, Das PK: Site of intimal rupture or erosion of thrombosed coronary atherosclerotic plaques is characterized by an inflammatory process irrespective of the dominant plaque morphology. Circulation 1994; 89: 36–44.
8. Moreno PR, Falk E, Palacios IF, Newell JB, Fuster V, Fallon JT: Macrophage infiltration in acute coronary syndromes. Implications for plaque rupture. Circulation 1994; 90: 775–778.
9. Virmani R, Kolodgie FD, Burke AP, Farb A, Schwartz SM: Lessons from sudden coronary death: a comprehensive morphological classification scheme for atherosclerotic lesions. Arterioscler Thromb Vasc Biol 2000; 20: 1262–1275.
10. Burke AP, Farb A, Malcom GT, Liang YH, Smialek J, Virmani R: Coronary risk factors and plaque morphology in men with coronary disease who died suddenly. N Engl J Med 1997; 336: 1276–1282.
11. Varnava AM, Mills PG, Davies MJ: Relationship between coronary artery remodeling and plaque vulnerability. Circulation 2002; 105: 939–943.
12. Suh WM, Seto AH, Margey RJ, Cruz-Gonzalez I, Jang IK: Intravascular detection of the vulnerable plaque. Circ Cardiovasc Imaging 2011; 4: 169–178.
13. Mintz GS, Nissen SE, Anderson WD, et al.: American College of Cardiology Clinical Expert Consensus Document on Standards for Acquisition, Measurement and Reporting of Intravascular Ultrasound Studies (IVUS). A report of the American College of Cardiology Task Force on Clinical Expert Consensus Documents. J Am Coll Cardiol 2001; 37: 1478–1492.
14. Yamagishi M, Terashima M, Awano K, et al.: Morphology of vulnerable coronary plaque: insights from follow-up of patients examined by intravascular ultrasound before an acute coronary syndrome. J Am Coll Cardiol 2000; 35: 106–111.
15. von Birgelen C, Klinkhart W, Mintz GS, et al.: Plaque distribution and vascular remodeling of ruptured and nonruptured coronary plaques in the same vessel: an intravascular ultrasound study *in vivo*. J Am Coll Cardiol 2001; 37: 1864–1870.
16. Low AF, Kawase Y, Chan YH, Tearney GJ, Bouma BE, Jang IK: *In vivo* characterisation of coronary plaques with conventional grey-scale intravascular ultrasound: correlation with optical coherence tomography. EuroIntervention 2009; 4: 626–632.
17. Moore MP, Spencer T, Salter DM, et al.: Characterisation of coronary atherosclerotic morphology by spectral analysis of radiofrequency signal: *in vitro* intravascular ultrasound study with histological and radiological validation. Heart 1998; 79: 459–467.
18. Okubo M, Kawasaki M, Ishihara Y, et al.: Tissue characterization of coronary plaques: comparison of integrated backscatter intravascular ultrasound with virtual histology intravascular ultrasound. Circ J 2008; 72: 1631–1639.
19. Nair A, Kuban BD, Tuzcu EM, Schoenhagen P, Nissen SE, Vince DG: Coronary plaque classification with intravascular ultrasound radiofrequency data analysis. Circulation 2002; 106: 2200–2206.
20. Nasu K, Tsuchikane E, Katoh O, et al.: Accuracy of *in vivo* coronary plaque morphology assessment: a validation study of *in vivo* virtual histology compared with *in vitro* histopathology. J Am Coll Cardiol 2006; 47: 2405–2412.
21. Toi T, Taguchi I, Yoneda S, et al.: Early effect of lipid-lowering therapy with pitavastatin on regression of coronary atherosclerotic plaque. Comparison with atorvastatin. Circ J 2009; 73: 1466–1472.
22. Kawaguchi R, Oshima S, Jingu M, et al.: Usefulness of virtual histology intravascular ultrasound to predict distal embolization for ST-segment elevation myocardial infarction. J Am Coll Cardiol 2007; 50: 1641–1646.
23. Rodriguez-Granillo GA, Garcia-Garcia HM, Mc Fadden EP, et al.: *In vivo* intravascular ultrasound-derived thin-cap fibroatheroma detection using ultrasound radiofrequency data analysis. J Am Coll Cardiol 2005; 46: 2038–2042.
24. Kubo T, Nakamura N, Matsuo Y, et al.: Virtual histology intravascular ultrasound compared with optical coherence tomography for identification of thin-cap fibroatheroma. Int Heart J 2011; 52: 175–179.
25. Hong MK, Mintz GS, Lee CW, et al.: Comparison of virtual histology to intravascular ultrasound of culprit coronary lesions in acute coronary syndrome and target coronary lesions in stable angina pectoris. Am J Cardiol 2007; 100: 953–959.
26. Nakamura T, Kubo N, Funayama H, Sugawara Y, Ako J, Momomura S: Plaque characteristics of the coronary segment proximal to the culprit lesion in stable and unstable patients. Clin Cardiol 2009; 32: E9–12.
27. Stone GW, Maehara A, Lansky AJ, et al.: A prospective natural-history study of coronary atherosclerosis. N Engl J Med 2011; 364: 226–235.
28. Kawasaki M, Takatsu H, Noda T, et al.: *In vivo*

quantitative tissue characterization of human coronary arterial plaques by use of integrated backscatter intravascular ultrasound and comparison with angioscopic findings. Circulation 2002; 105: 2487–2492.
29. Kawasaki M, Bouma BE, Bressner J, et al.: Diagnostic accuracy of optical coherence tomography and integrated backscatter intravascular ultrasound images for tissue characterization of human coronary plaques. J Am Coll Cardiol 2006; 48: 81–88.
30. Sano K, Kawasaki M, Ishihara Y, et al.: Assessment of vulnerable plaques causing acute coronary syndrome using integrated backscatter intravascular ultrasound. J Am Coll Cardiol 2006; 47: 734–741.
31. Ando H, Amano T, Matsubara T, et al.: Comparison of tissue characteristics between acute coronary syndrome and stable angina pectoris. An integrated backscatter intravascular ultrasound analysis of culprit and non-culprit lesions. Circ J 2011; 75: 383–390.
32. Takeuchi H, Morino Y, Matsukage T, et al.: Impact of vascular remodeling on the coronary plaque compositions: an investigation with *in vivo* tissue characterization using integrated backscatter-intravascular ultrasound. Atherosclerosis 2009; 202: 476–482.
33. Kawasaki M, Sano K, Okubo M, et al.: Volumetric quantitative analysis of tissue characteristics of coronary plaques after statin therapy using three-dimensional integrated backscatter intravascular ultrasound. J Am Coll Cardiol 2005; 45: 1946–1953.
34. Otagiri K, Tsutsui H, Kumazaki S, et al.: Early intervention with rosuvastatin decreases the lipid components of the plaque in acute coronary syndrome: analysis using integrated backscatter IVUS (ELAN study). Circ J 2011; 75: 633–641.
35. Mehta SK, McCrary JR, Frutkin AD, Dolla WJ, Marso SP: Intravascular ultrasound radiofrequency analysis of coronary atherosclerosis: an emerging technology for the assessment of vulnerable plaque. Eur Heart J 2007; 28: 1283–1288.
36. Kawano T, Honye J, Takayama T, et al.: Compositional analysis of angioscopic yellow plaques with intravascular ultrasound radiofrequency data. Int J Cardiol 2008; 125: 74–78.
37. Takano M, Jang IK, Inami S, et al.: *In vivo* comparison of optical coherence tomography and angioscopy for the evaluation of coronary plaque characteristics. Am J Cardiol 2008; 101: 471–476.
38. Yamamoto M, Takano M, Okamatsu K, et al.: Relationship between thin cap fibroatheroma identified by virtual histology and angioscopic yellow plaque in quantitative analysis with colorimetry. Circ J 2009; 73: 497–502.
39. Kubo T, Imanishi T, Takarada S, et al.: Implication of plaque color classification for assessing plaque vulnerability: a coronary angioscopy and optical coherence tomography investigation. JACC Cardiovasc Interv 2008; 1: 74–80.
40. Takano M, Mizuno K, Okamatsu K, Yokoyama S, Ohba T, Sakai S: Mechanical and structural characteristics of vulnerable plaques: analysis by coronary angioscopy and intravascular ultrasound. J Am Coll Cardiol 2001; 38: 99–104.
41. Sakai S, Mizuno K, Yokoyama S, et al.: Morphologic changes in infarct-related plaque after coronary stent placement: a serial angioscopy study. J Am Coll Cardiol 2003; 42: 1558–1565.
42. Okamatsu K, Takano M, Sakai S, et al.: Elevated troponin T levels and lesion characteristics in non-ST-elevation acute coronary syndromes. Circulation 2004; 109: 465–470.
43. Mizuno K, Satomura K, Miyamoto A, et al.: Angioscopic evaluation of coronary-artery thrombi in acute coronary syndromes. N Engl J Med 1992; 326: 287–291.
44. Mizuno K, Miyamoto A, Satomura K, et al.: Angioscopic coronary macromorphology in patients with acute coronary disorders. Lancet 1991; 337: 809–812.
45. Takano M, Inami S, Ishibashi F, et al.: Angioscopic follow-up study of coronary ruptured plaques in nonculprit lesions. J Am Coll Cardiol 2005; 45: 652–658.
46. Asakura M, Ueda Y, Yamaguchi O, et al.: Extensive development of vulnerable plaques as a pan-coronary process in patients with myocardial infarction: an angioscopic study. J Am Coll Cardiol 2001; 37: 1284–1288.
47. Uchida Y, Nakamura F, Tomaru T, et al.: Prediction of acute coronary syndromes by percutaneous coronary angioscopy in patients with stable angina. Am Heart J 1995; 130: 195–203.
48. Ohtani T, Ueda Y, Mizote I, et al.: Number of yellow plaques detected in a coronary artery is associated with future risk of acute coronary syndrome: detection of vulnerable patients by angioscopy. J Am Coll Cardiol 2006; 47: 2194–2200.
49. MacNeill BD, Lowe HC, Takano M, Fuster V, Jang IK: Intravascular modalities for detection of vulnerable plaque: current status. Arterioscler Thromb Vasc Biol 2003; 23: 1333–1342.
50. Inami S, Ishibashi F, Waxman S, et al.: Multiple yellow plaques assessed by angioscopy with quantitative colorimetry in patients with myocardial infarction. Circ J 2008; 72: 399–403.
51. Lehmann KG, van Suylen RJ, Stibbe J, et al.: Composition of human thrombus assessed by quantitative colorimetric angioscopic analysis. Circulation 1997; 96: 3030–3041.
52. Ishibashi F, Mizuno K, Kawamura A, Singh PP, Nesto RW, Waxman S: High yellow color intensity by angioscopy with quantitative colorimetry to identify high-risk features in culprit lesions of patients with acute coronary syndromes. Am J Cardiol 2007; 100: 1207–1211.
53. Uchida Y, Kawai S, Kanamaru R, et al.: Detection of vulnerable coronary plaques by color fluorescent angioscopy. JACC Cardiovasc Imaging 2010; 3: 398–408.
54. Yabushita H, Bouma BE, Houser SL, et al.: Characterization of human atherosclerosis by optical coherence tomography. Circulation 2002; 106: 1640–1645.
55. Jang IK, Bouma BE, Kang DH, et al.: Visualization of coronary atherosclerotic plaques in patients using optical coherence tomography: comparison with intravascular ultrasound. J Am Coll Cardiol 2002; 39: 604–609.

56. Kubo T, Imanishi T, Takarada S, et al.: Assessment of culprit lesion morphology in acute myocardial infarction: ability of optical coherence tomography compared with intravascular ultrasound and coronary angioscopy. J Am Coll Cardiol 2007; 50: 933–939.
57. Jang IK, Tearney GJ, MacNeill B, et al.: *In vivo* characterization of coronary atherosclerotic plaque by use of optical coherence tomography. Circulation 2005; 111: 1551–1555.
58. Kume T, Akasaka T, Kawamoto T, et al.: Assessment of coronary arterial plaque by optical coherence tomography. Am J Cardiol 2006; 97: 1172–1175.
59. Tanaka A, Imanishi T, Kitabata H, et al.: Lipid-rich plaque and myocardial perfusion after successful stenting in patients with non-ST-segment elevation acute coronary syndrome: an optical coherence tomography study. Eur Heart J 2009; 30: 1348–1355.
60. Yonetsu T, Kakuta T, Lee T, et al.: Impact of plaque morphology on creatine kinase-MB elevation in patients with elective stent implantation. Int J Cardiol 2011; 146: 80–85.
61. Lee T, Yonetsu T, Koura K, et al.: Impact of Coronary Plaque Morphology Assessed by Optical Coherence Tomography on Cardiac Troponin Elevation in Patients With Elective Stent Implantation. Circ Cardiovasc Interv 2011; 4: 378–386.
62. Kume T, Akasaka T, Kawamoto T, et al.: Assessment of coronary arterial thrombus by optical coherence tomography. Am J Cardiol 2006; 97: 1713–1717.
63. Meng L, Lv B, Zhang S, Yv B: *In vivo* optical coherence tomography of experimental thrombosis in a rabbit carotid model. Heart 2008; 94: 777–780.
64. Tearney GJ, Yabushita H, Houser SL, et al.: Quantification of macrophage content in atherosclerotic plaques by optical coherence tomography. Circulation 2003; 107: 113–119.
65. Kolodgie FD, Gold HK, Burke AP, et al.: Intraplaque hemorrhage and progression of coronary atheroma. N Engl J Med 2003; 349: 2316–2325.
66. Moreno PR, Purushothaman KR, Fuster V, et al.: Plaque neovascularization is increased in ruptured atherosclerotic lesions of human aorta: implications for plaque vulnerability. Circulation 2004; 110: 2032–2038.
67. Kitabata H, Tanaka A, Kubo T, et al.: Relation of microchannel structure identified by optical coherence tomography to plaque vulnerability in patients with coronary artery disease. Am J Cardiol 2010; 105: 1673–1678.
68. Manfrini O, Mont E, Leone O, et al.: Sources of error and interpretation of plaque morphology by optical coherence tomography. Am J Cardiol 2006; 98: 156–159.

(Received, September 7, 2011)
(Accepted, September 26, 2011)